PARAMETER
JURNAL MATEMATIKA, STATISTIKA DAN TERAPANNYA

e-ISSN. 2829-6303
Vol. 05, No. 2, September 2026
Pages 345-360

Check for updates

Probabilistic Seismic Hazard Assessment of Southern Offshore East Java Using Poisson and Gutenberg–Richter Models

Ajril Abyad Al Haq[1*], Eriska Fitri Kurniawati[2]

[1,2]Department of Mathematics, Faculty of Mathematics and Natural Sciences,
Universitas PGRI Ronggolawe
Jalan Manunggal No. 61, Tuban, 62381, Jawa Timur, Indonesia

E-mail Correspondence Author: *abyadalhaq02@gmail.com

Abstract

The southern offshore of East Java, situated along the active Sunda Subduction Zone, faces significant seismic threats from the convergence of the Indo-Australian and Eurasian Plates. This study evaluates earthquake probabilities in this region (8.5°S–12°S, 110°E–115°E) by combining the Gutenberg–Richter law with a stationary Poisson model. Seismicity data from the International Seismological Centre (1996–2025) were declustered using the Gardner and Knopoff method, yielding 1,348 mainshocks. A corrected completeness magnitude ($M_C = 4.2$) *filtered the catalog into a robust dataset of 888 events* ($\bar{M} = 4.51$). *The estimated seismic parameters* ($a = 7.970877$), ($b = 1.195825$) *indicate a highly productive tectonic environment dominated by small-to-moderate events. The Kolmogorov–Smirnov test validated the stationary Poisson model* ($D_{\text{calculated}} = 0.204086 \leq D_{\text{table}} = 0.297595$) *for annual mainshock counts. Temporal extrapolations indicate high seismic hazards over a 50-year horizon, with occurrence probabilities of 92.78% for* $M \geq 6.5$, *15.42% for* $M \geq 7.5$, *and 1.06% for a megathrust event* ($M \geq 8.5$). *These estimates provide a verified quantitative foundation for updating building codes and engineering practices along East Java's vulnerable coastline.*

Keywords: *Earthquake probability, gutenberg–richter law, poisson distribution, seismic hazard.*

: https://doi.org/10.30598/parameterv5i2pp345-360

This article is an open access article distributed under the terms and conditions of the Creative Commons Attribution-ShareAlike 4.0 International License.

Copyright © 2026 The Author(s).
Research Ariticle ***Open Acces***
Email: jurnalparameter@gmail.com
Homepage: https://ojs3.unpatti.ac.id/index.php/parameter

Submitted: May 2026
Accepted: September 2026

1. INTRODUCTION

Indonesia is considered one of the most tectonically active regions in the world because it lies at the junction of three major tectonic plates: the Eurasian, Pacific, and Indo-Australian plates [1]. This geographical setting makes most of Indonesia, including southern East Java, highly vulnerable to earthquakes. Specifically, the southern region of East Java is part of the Sunda subduction zone, where the Indo-Australian Plate is slowly subducting beneath the Eurasian Plate. It is this process that, over the years, has triggered the accumulation of tectonic energy and released it in the form of moderate- to large-magnitude earthquakes[2].

The history of Indonesia records several major earthquakes that have struck the region as a result of this subduction activity. In 2004, Aceh was struck by a devastating earthquake with a magnitude of over 9 Mw, followed by a tsunami, claiming hundreds of thousands of lives [3]. Similar events, albeit on a different scale, have also occurred in southern Java. The 2006 Pangandaran earthquake accompanied by a tsunami, the Yogyakarta earthquake in the same year, and the 2021 southern Malang earthquake serve as clear evidence that the southern Java region harbors seismic threats that cannot be ignored [4], [5]. Continuous seismic activity along the Sunda subduction zone indicates that the potential for a major earthquake in the future remains high. The Indo-Australian Plate moves at a certain speed each year, causing tectonic energy to continue to build up [6]. If this energy is not released periodically through small or moderate earthquakes, a major earthquake is highly likely one that could even trigger a tsunami, as occurred in Aceh and Pangandaran [7]. Based on data from the International Seismological Centre (ISC) earthquake catalog for the period 1996–2025, thousands of earthquakes with magnitudes above 4.0 have been recorded in the southern part of East Java. This figure further underscores the high level of seismic risk in the region.

The risk of earthquakes is certainly a serious concern, especially for communities living in the southern coastal region of East Java [8]. For this reason, systematic efforts are needed to assess the likelihood of an earthquake of a certain magnitude occurring within a specific time frame. One widely used approach in seismic hazard studies is earthquake probability analysis through a combination of the Gutenberg–Richter law and the Poisson model. This approach can estimate the probability of an earthquake occurring across various magnitude ranges and time periods [9]. There are two important parameters in the Gutenberg–Richter law parameters a and b which can provide insight into a region's level of seismic activity as well as the prevailing tectonic stress conditions [10].

Against this background, this study aims to analyze the probability of earthquake occurrence in the southern offshore region of East Java using the Poisson model and the Gutenberg–Richter law, based on ISC earthquake catalog data for the period 1996–2025. Specifically, this study estimates the likelihood of earthquakes with magnitudes ≥6.5, ≥7.5, and ≥8.5 occurring across various time horizons, with the goal of providing a quantitative foundation for disaster mitigation and regional planning in the southern coastal area of East Java. Previous studies in East Java have addressed seismic hazard from various angles. Fitria and Prastowo [11] analyzed the seismicity of East Java and its associated seismic hazard potential. Anggarajati et al. [5] mapped earthquake-prone zones across Java Island using K-means clustering combined with b-value analysis. Rahmatullah et al. [6] developed a peak ground motion acceleration map for Surabaya City based on probabilistic seismic hazard analysis (PSHA). Meanwhile, Firdaus and Maulana [12] modeled earthquakes in East Java Province using extreme value theory combined with PSHA. However, these studies generally adopt a fixed minimum

magnitude as an arbitrary threshold without rigorously determining the Magnitude of Completeness (M_C). Unlike them, this study rigorously determines M_C using the Maximum Curvature (MAXC) method with a +0.2 correction. Although this correction is well established in global seismological literature, its application for determining M_C in the southern East Java subduction segment has — to the best of the authors' knowledge — not been specifically reported, making the present study a regionally novel contribution.

2. METHOD

This study uses secondary data from the ISC (International Seismological Centre) earthquake catalog for the southern region of East Java at coordinates 8.5°S to 12°S (South Latitude) and 110°E to 115°E (East Longitude). This region is an active subduction zone between the Indo-Australian Plate and the Eurasian Plate, characterized by high seismicity. The research was conducted through the following systematic stages.

2.1. Gathering Data

The earthquake data were obtained from the International Seismological Centre (ISC) via the ISC's official website [13], with the study area bounded by coordinates 8.5°S to 12°S and 110°E to 115°E. The downloaded data include the time of occurrence, epicenter coordinates, magnitude type (mb), and depth, covering the period from 1996 to 2025. Only earthquakes with a minimum magnitude of 4.0 and depths ranging from 10 to 100 km were selected, as events within this depth range have the potential to damage infrastructure, trigger tsunamis, or cause other types of hazards.

2.2. Declustering data

Earthquake data were then declustered using the method developed by Gardner and Knopoff (1974) [14]. This step aims to separate the mainshock from the aftershocks, since the Poisson model assumes that earthquake events are independent of one another. Only the mainshock was used in subsequent analyses.

2.3. Calculation of Magnitude of Completeness (M_C) and Average Magnitude ($\bar{M}$)

The Magnitude of Completeness (M_C) is determined using the Maximum Curvature (MAXC) method [15], which is the magnitude value with the highest frequency in the magnitude distribution histogram::

$$M_C = \text{argmax}\,(f(M)) \tag{1}$$

Because the MAXC method tends to produce M_C values that are too low [16], a correction was made by adding 0.2 [17]. To avoid bias in the statistical analysis:

$$M_{C(correction)} = M_C + 0.2 \tag{2}$$

Once M_C has been determined, the next step is to calculate the average magnitude ($\bar{M}$) for all earthquakes with a magnitude greater than or equal to M_C:

$$\bar{M} = \frac{1}{n}\sum_{i=1}^{1} Mi \tag{3}$$

where n is the number of earthquakes with $Mi \geq M_C$

2.4. Normality Test (Kolmogorov-Smirnov)

The Kolmogorov-Smirnov test was used to determine whether the annual counts of mainshock events follow a Poisson distribution, consistent with the standard assumption that the number of earthquakes per unit time interval in a Poisson process is itself Poisson-distributed [18]. This test compares the empirical cumulative distribution function ($F_n(x)$) with the theoretical Poisson cumulative distribution function ($F(x)$) [19], [20].

$$D = \sup_{x} |F_n(x) - F(x)| \tag{4}$$

Hypothesis:

H_0 : The data follow a Poisson distribution

H_1 : The data do not follow a Poisson distribution

Criteria:

If $D \leq 1.63/\sqrt{T}$ or $p > 0.01$, then H_0 accepted.

If $D > 1.63/\sqrt{T}$ or $p \leq 0.01$,then H_0 rejected.

where T is the number of years of observation.

However, if H_0 is rejected, the Poisson model can still be used as a conservative estimate.

2.5. Parametric Estimation of b Using the Aki 1965 Method

Parameter b is estimated using the Aki (1965) method [21]:

$$b = \frac{\log_{10} e}{\bar{M} - \left(M_c - \frac{\Delta M}{2}\right)} \tag{5}$$

where $\log_{10} e = 0.434294$, $\bar{M}$ is the average magnitude of earthquakes above M_C, and $\Delta M = 0.1$ (magnitude interval).

Interpretation of the value of b [22]:

$b < 1$: High potential for major earthquakes

$b > 1$: Predominance of minor earthquakes

$b \approx 1$: Balance between minor and major earthquakes

2.6. Parametric Estimation of a Using the Gutenberg-Richter Equation

The parameter a in the Gutenberg–Richter law is calculated using the formula [23]:

$$a = \log_{10} N + bM_C \tag{6}$$

with:

N = Total number of earthquakes with a magnitude $\geq M_C$

b = Aki (1965) estimated parameter

The parameter *a* reflects the level of seismic activity in a region. The larger the value of *a*, the higher the seismic activity in that region [24].

2.7. Probability Calculation of Earthquakes Using the Poisson Model

The probability of an earthquake occurring is calculated using the Poisson distribution, as applied to seismic hazard analysis by Cornell (1968) [25]. The probability of at least one earthquake occurring within a time period of t years is [26]:

$$P(N \geq 1) = 1 - e^{-\lambda t} \tag{7}$$

with:

λ = annual occurrence rate for a given magnitude

t = the time period under consideration (1, 5, 10, 25, 50, and 100 years)

The value of λ for each magnitude threshold ($M \geq 6.5$, $M \geq 7.5$, and $M \geq 8.5$) is derived from the Gutenberg–Richter relationship.

3. RESULTS AND DISCUSSION

3.1. Data declustering process

Earthquake data were retrieved from the International Seismological Centre (ISC) online database for the region bounded by coordinates 8.5°S to 12°S (South Latitude) and 110°E to 115°E (East Longitude), initially yielding 1,699 raw seismic events. From this dataset, 351 events identified as aftershocks were removed using the Gardner and Knopoff declustering method.. As a result, 1,348 events remained as mainshocks over a 30-year period, from 1996 to 2025. The lowest number of events was recorded in 2002, with only 19 events, while the highest peak of activity occurred in 2017 with 87 events. Overall, the average number of major earthquakes per year in this region is approximately 44.9 events per year. This figure is relatively high and confirms that the southern part of East Java is a highly tectonically active region, given its location at the boundary between the Indo-Australian Plate and the Eurasian Plate. The annual distribution of major earthquake events is presented in **Table 1**.

Table 1. Number of Major Earthquakes per Year (1996–2025)

No	Year	Incident	No	Year	Incident
1	1996	41	16	2011	44
2	1997	34	17	2012	50
3	1998	24	18	2013	49
4	1999	40	19	2014	59
5	2000	29	20	2015	57
6	2001	36	21	2016	62
7	2002	19	22	2017	87
8	2003	26	23	2018	78
9	2004	44	24	2019	79
10	2005	35	25	2020	63
11	2006	29	26	2021	51
12	2007	29	27	2022	53
13	2008	37	28	2023	54
14	2009	27	29	2024	39
15	2010	44	30	2025	29
Total Incident					1,348

Table 1 shows the data after the declustering process, which involves separating the aftershocks from the mainshock. Once the declustering is complete, determine the Magnitude of Completeness (M_C).

3.2. Determining the Magnitude of Completeness (M_C) and $\bar{M}$

When determining M_C, we can visualize the earthquake data by plotting the number of earthquake events within a specific magnitude range in the collected data. As shown in **Figure 1**.

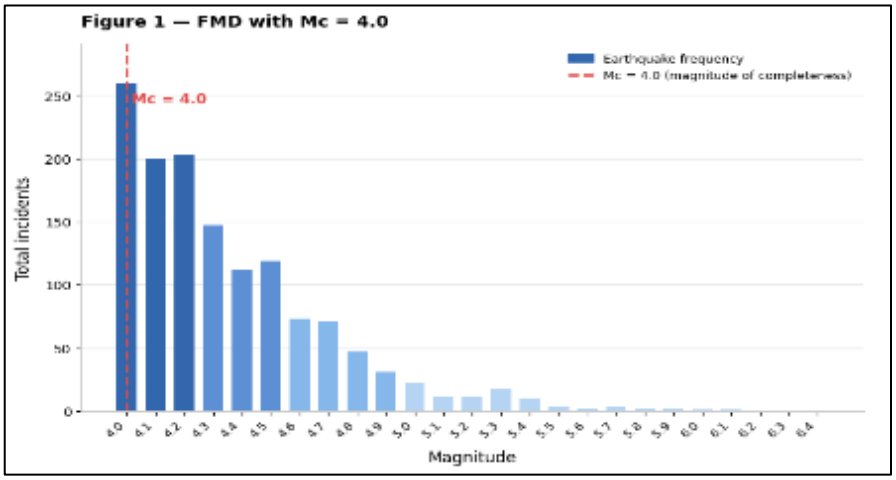


Figure 1. Frequency-Magnitude Distribution (FMD) with a magnitude of $M_C = 4.0$

Figure 1 presents the frequency-magnitude distribution (FMD) of the earthquake catalog for the study area, where the horizontal axis represents magnitude classes (M 4.0–6.4) and the vertical axis represents the number of events in each class. Out of 1,348 total events, the highest frequencies were observed at M 4.0 and M 4.1 with 260 and 200 events respectively, declining exponentially with increasing magnitude in accordance with the Gutenberg-Richter law. The initial completeness magnitude (M_C) was set at M 4.0; however, a correction of +0.2 was applied considering the potential underreporting at the lowest magnitude classes, yielding a revised M_C of 4.2, as illustrated in **Figure 2**, which was subsequently used as the lower bound for further analysis.

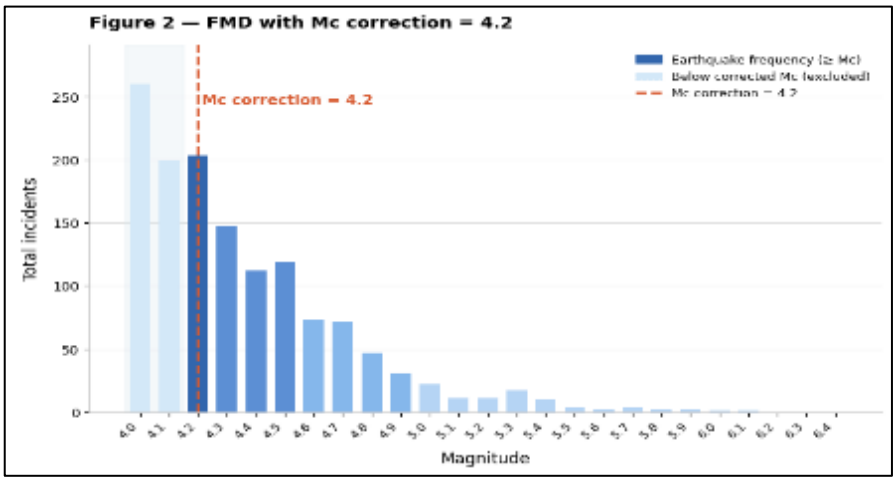


Figure 2. Frequency-Magnitude Distribution (FMD) with $M_{C(correction)} = 4.2$

Figure 2 presents the frequency-magnitude distribution (FMD) following the correction of the Magnitude of Completeness (M_C) value from 4.0 to 4.2. In this visualization, the light blue bars represent earthquake events with magnitudes of 4.0 and 4.1, which were considered potentially incomplete and therefore excluded from further analysis. Meanwhile, the dark blue bars correspond to magnitudes of 4.2 and above, which were retained as completely recorded events. The red dashed line vertically marks the corrected completeness threshold at $M_C = 4.2$, clearly separating the excluded data from the data used in the b-value calculation. As a result, out of a total of 1,348 earthquake events that had previously undergone the declustering process, only 888 events with magnitudes of 4.2 and above—averaging 29.6 events per year—were utilized in the

Gutenberg–Richter relationship. This approach ensures a more representative and unbiased estimation of the b-value, free from the influence of incomplete catalog entries.

Once the completeness magnitude (M_C) was established, the mean magnitude ($\bar{M}$) was computed for all events with $M_i \geq M_C$. Given that the data are presented in the form of a frequency distribution, $\bar{M}$ was calculated as the sum of the product of each magnitude value and its corresponding frequency, divided by the total number of events.

$$\bar{M} = \frac{\sum_{i=1}^{k}(M_i \times n_i)}{N_{Total}} \tag{8}$$

Based on this formula , the frequency distribution of magnitudes for earthquakes with $M \geq M_C$ is presented in **Table 2** below. The first column shows the magnitude values, the second column shows the number of occurrences (frequency), and the third column contains the product of magnitude and frequency, which is used to calculate $\bar{M}$.

Table 2. Frequency Distribution of Earthquake Magnitudes with $M \geq M_C$

M_i (Magnitude)	n_i (Incident)	$M_i \times n_i$
4.2	203	852.6
4.3	147	632.1
4.4	112	492.8
4.5	119	535.5
4.6	73	335.8
4.7	71	333.7
4.8	47	225.6
4.9	31	151.9
5	22	110.0
5.1	11	56.1
5.2	11	57.2
5.3	17	90.1
5.4	10	54.0
5.5	3	16.5
5.6	2	11.2
5.7	3	17.1
5.8	2	11.6
5.9	2	11.8
6	1	6
6.1	1	6
6.2	0	0
6.3	0	0
6.4	0	0
Total	888	4007.7

Table 2 presents data on earthquake magnitude (M_i), the number of events (n_i), and the product of magnitude and frequency ($M_i \times n_i$), which are used to calculate the average magnitude ($\bar{M}$).

$$\bar{M} = \frac{\sum_{i=1}^{k}(M_i \times n_i)}{N_{Total}} = \frac{4007.7}{888}$$

$$\bar{M} = 4.513176$$

The value is $\bar{M} = 4.51$, the average earthquake magnitude used to calculate the parameter b in the Gutenberg–Richter law.

3.3. Kolmogorov-Smirnov Test for Annual Mainshock Counts

The Kolmogorov-Smirnov (KS) test was deployed to evaluate whether the annual counts of mainshock events follow a stationary Poisson distribution. This statistical validation explicitly addresses the requirement of a constant occurrence rate over the 30-year observation window, alongside the independence achieved through declustering. The following hypotheses were tested:

H_0: The data follow a Poisson distribution

H_1: The data do not follow a Poisson distribution

The results of the Kolmogorov-Smirnov (KS) test are presented in **Table 3**. This test aims to verify whether the annual mainshock event data in the southern region of East Java follow a Poisson distribution. The hypotheses proposed are H_0: the data follow a Poisson distribution, and H_1: the data do not follow a Poisson distribution. The test was conducted by comparing the empirical cumulative distribution function of the actual data with the theoretical cumulative distribution function of the Poisson distribution. The critical value DtableDtable was calculated based on the number of observation years ($T = 30$) with a significance level of $\alpha = 0.01$.

Table 3. Kolmogorov-Smirnov Test Results for Annual Earthquake Occurrence Data

No	Year	Incident	F_{Cum}	F_{Teo} Poisson	ABS F_{Cum} - F_{Teo}
1	2002	10	0.033333	0.000029	0.033304
2	2007	14	0.066667	0.001149	0.065517
3	2009	16	0.100000	0.004719	0.095281
4	2006	17	0.133333	0.008753	0.124580
5	2003	19	0.166667	0.025723	0.140944
6	1997	20	0.200000	0.041020	0.158981
7	1998	21	0.233333	0.062580	0.170753
8	**2008**	**21**	**0.266667**	**0.062580**	**0.204086 ($D_{calculated}$)**
9	2025	25	0.300000	0.229484	0.070516
10	1996	26	0.333333	0.291550	0.041784
11	2000	26	0.366667	0.291550	0.075117
12	2010	26	0.400000	0.291550	0.108451
13	2001	28	0.433333	0.431522	0.001812
14	2011	28	0.466667	0.431522	0.035145
15	2012	28	0.500000	0.431522	0.068479
16	2024	28	0.533333	0.431522	0.101812
17	2004	29	0.566667	0.504940	0.061727
18	2005	29	0.600000	0.504940	0.095060
19	2013	31	0.633333	0.646547	0.013214
20	1999	32	0.666667	0.710528	0.043861
21	2022	32	0.700000	0.710528	0.010528
22	2014	34	0.733333	0.817878	0.084545
23	2016	34	0.766667	0.817878	0.051211
24	2020	34	0.800000	0.817878	0.017878
25	2021	35	0.833333	0.860131	0.026798
26	2015	36	0.866667	0.894873	0.028206
27	2023	39	0.900000	0.960747	0.060747
28	2018	50	0.933333	0.999779	0.066446
29	2019	53	0.966667	0.999964	0.033297
30	2017	67	1	1	0

Based on **Table 3**, the calculated Kolmogorov-Smirnov statistic is $D_{calculated} = 0.204086$, which represents the maximum value from the absolute difference column. The critical value D_{Tabel} at a significance level of $\alpha = 0.01$ for $T = 30$ observation years is:

$$D_{Tabel} = \frac{1.63}{\sqrt{T}} = \frac{1.63}{\sqrt{30}} = 0.297595 \quad (9)$$

Because $D_{Calculated} = 0.204086$ is less than or equal to the critical value $D_{Tabel} = 0.297595$, we accept H_0 at the 1% significance level. This result formally confirms that the annual mainshock counts follow a Poisson distribution, aligning with the theoretical expectation that event frequencies per fixed time interval in a Poisson process are Poisson-distributed. Consequently, the stationary Poisson model is validated as methodologically sound and highly suitable for estimating the probabilistic seismic hazard in this region.

3.4. *b*-value Estimation using the Aki 1965 Method

Once the values of $M_C = 4.2$ and $\bar{M} = 4.51$ were obtained, the b-value was estimated using the Aki 1965 method as shown in **Equation (5)**:

$$b = \frac{\log_{10} e}{\bar{M} - \left(M_c - \frac{\Delta M}{2}\right)}$$

$$b = \frac{0.434294}{4.51 - \left(4.2 - \frac{0.1}{2}\right)} = 1.195825$$

With a *b*-value of 1.195825, the southern region of East Java is characterized by a predominance of small to moderate magnitude earthquakes, since a b-value greater than 1 physically indicates a higher frequency of small events compared to larger ones. Nevertheless, the potential for a major earthquake cannot be ruled out, as tectonic energy continues to accumulate within the Sunda Subduction Zone.

3.5. *a*-value Estimation using the Gutenberg–Richter Law

Once the *b*-value and M_C were obtained, the *a*-value was estimated using the Gutenberg–Richter law as shown in **Equation (6)**:

$$a = \log_{10} N + bM_C$$

$$a = \log_{10}(888) + (1.195825 \times 4.2) = 7.970877$$

The *a*-value of 7.970877 indicates that the southern region of East Java has a high level of seismic productivity. This is consistent with the tectonic condition of the region, which lies within the Sunda Subduction Zone, where the subduction activity of the Indo-Australian Plate beneath the Eurasian Plate takes place continuously.

3.6. Probability of Earthquake Occurrence Using the Poisson Model

3.6.1. Extrapolation of Annual Occurrence Rate (λ)

Because no earthquakes with a magnitude of $M \geq 6.5$ were recorded during the 30-year observation period, the annual occurrence rate (λ) for each magnitude threshold was derived by extrapolating the Gutenberg–Richter relationship using the estimated parameters $a = 7.970877$ and $b = 1.195825$. The following steps illustrate the calculation for the $M \geq 6.5$ threshold using the Gutenberg–Richter equation **[23]**:

$$\log_{10} N = a - bM \tag{10}$$

Substituting the values of $a = 7.970877$, $b = 1.195825$, and $M = 6.5$:

$$\log_{10} N = 7.970877 - (1.195825 \times 6.5) = 0.198016$$

The number of events N over 30 years is then obtained by:

$$N = 10^{0.198016} = 1.577669$$

Once the value $N = 1.577669$ is obtained, representing the number of events within the 30-year period, the next step is to determine λ, the annual occurrence rate. The annual occurrence rate λ is calculated using **Equation (11)**:

$$\lambda = \frac{N}{T} \tag{11}$$

Substituting the values of $N = 1.577669$ and $T = 30$ years:

$$\lambda = \frac{1.577669}{30} = 0.052589 \text{ events/year}$$

3.6.2. Probability Calculation for $M \geq 6.5$

Furthermore, the probability of at least one earthquake occurring within a time period of t years is calculated using the Poisson model, as shown in **Equation (7)**:

$$P(N \geq 1) = 1 - e^{-\lambda t}$$

For illustration, taking $t = 50$ years:

$$P(N \geq 1) = 1 - e^{-\lambda t} = 1 - e^{-0.052589 \times 50} = 0.927882 \ (92.78\%)$$

3.6.3. Probability Results for All Magnitude Thresholds

Using the same procedure, extrapolations were performed for magnitude thresholds $M \geq 7.5$ and $M \geq 8.5$. The complete calculation results for N (number of events over 30 years) and λ (annual occurrence rate) for all three thresholds are presented in **Table 4**.

Table 4. Complete Calculation Results for Each Magnitude Threshold

M	$\log_{10} N$	N (30 year)	λ (per year)
6.5	0.198016	1.577669	0.052589
7.5	-0.997809	0.100506	0.003350
8.5	-2.193634	0.006403	0.000213

Table 4 demonstrates that increasing the magnitude threshold exponentially results in smaller N and λ values, adhering strictly to the Gutenberg–Richter law. It is critical to note that while the $\log_{10} N$ column exhibits negative values (e.g., -0.997809 for $M \geq 7.5$), this is mathematically expected in logarithmic transformations when the extrapolated cumulative frequency N falls below 1, and does not represent a negative count of physical events. When compared to adjacent tectonic segments, the calculated b-value of 1.195825 in the southern offshore of East Java indicates a relatively higher proportion of small-to-moderate seismic events compared to the deeper subduction segments of western Sumatra, where b-values often hover around 0.8 to 1.0 due to higher

structural locking and stress accumulation. However, this high seismic productivity (reflected by $a = 7.970877$) closely aligns with probabilistic seismic hazard assessments conducted along the broader Sunda Subduction Zone, confirming that while energy is frequently released through smaller earthquakes, the continuous plate convergence maintains a significant long-term megathrust hazard for the southern coastal region of Java. The λ values presented in **Table 4** were then used to estimate the probability of at least one earthquake event occurring over different time periods using the Poisson model. For instance, for $M \geq 6.5$ with an annual occurrence rate of $\lambda = 0.052589$ events per year, the probability of an earthquake occurring within 50 years is approximately 92.78%. For $M \geq 7.5$, with $\lambda = 0.003350$ events per year, the probability within 50 years is 15.42%. Meanwhile, for $M \geq 8.5$, with $\lambda = 0.000213$ events per year, the probability within 50 years is only 1.06%. A complete summary of the probability results for all three magnitude thresholds and various time periods is provided in **Table 5**.

Table 5. Earthquake Probability by Magnitude and Time

Year	$M \geq 6.5$	$M \geq 7.5$	$M \geq 8.5$
1	0.051230	0.003345	0.000213
5	0.231216	0.016611	0.001067
10	0.408971	0.032947	0.002132
25	0.731452	0.080343	0.005321
50	0.927882	0.154232	0.010615
100	0.994799	0.284676	0.021116

To better illustrate the trend of increasing probability over time, the results from **Table 5** are also presented graphically in **Figure 3**.

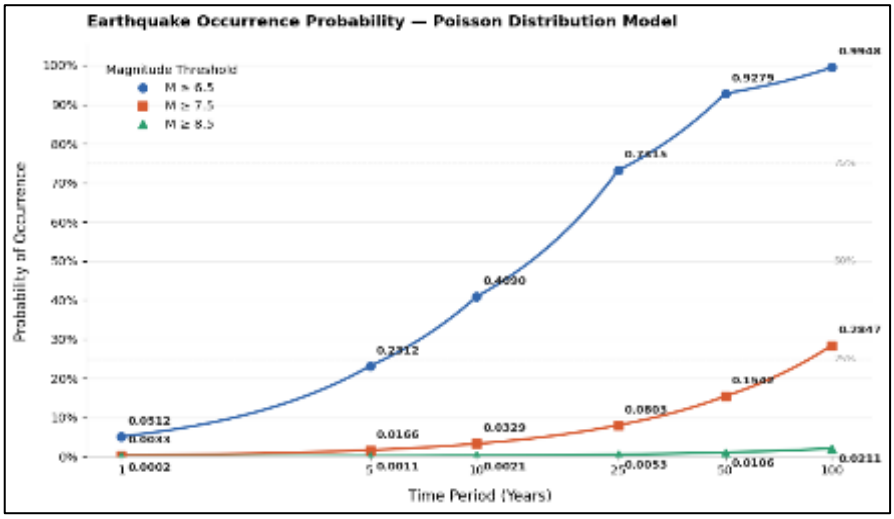


Figure 3. Earthquake probability trends for different magnitude thresholds (1–100 years)

Based on **Table 5** and **Figure 3**, for $M \geq 6.5$, the probability of an earthquake occurring within 50 years reaches 92.78%, and within 100 years, it increases to 99.48%. These figures indicate that the threat of moderate to large earthquakes in the southern region of East Java is very high. For $M \geq 7.5$, the probability within 50 years is 15.42%, and within 100 years, it reaches 28.47%. Meanwhile, for $M \geq 8.5$, the probability within 50 years is only 1.06%, and within 100 years, it is 2.11%. Although the probability of a megathrust earthquake ($M \geq 8.5$) is relatively small, its extreme impact (such as a tsunami) cannot be ignored. These results confirm that the southern coastal region of

East Java requires a high level of preparedness and well-planned disaster mitigation strategies.

The M_C value of 4.2, determined using the MAXC method with a +0.2 correction following Woessner and Wiemer [17], ensures only statistically complete data were analyzed, consistent with completeness frameworks proposed by Wang et al. [15] and Pavlenko and Zavyalov [16]. The Kolmogorov–Smirnov test, as applied by Li et al. [18], Drajati and Roshafara [19], and Yang et al. [20], confirmed that the annual mainshock counts data follow a Poisson distribution ($D_{calculated} = 0.204086 \leq D_{table} = 0.297595$), validating the applied probability model. The b-value of 1.195825 is consistent with Anggarajati et al. [5], who identified elevated b-values across Java, while the high a-value aligns with probabilistic ground motion assessments by Rahmatullah et al. [6] for the Surabaya region, collectively reinforcing the substantial seismic threat of the southern East Java segment. These findings further support the characterization of the Sunda subduction zone as a highly active tectonic environment documented by Zhou and Xia [9], underscoring the urgency of incorporating long-term probabilistic seismic hazard estimates into regional disaster mitigation frameworks.

This study has several limitations. First, no earthquakes with magnitudes ≥ 6.5 were recorded during the 30-year observation period, so the probabilities for $M \geq 6.5$, $M \geq 7.5$, and $M \geq 8.5$ were obtained through extrapolation rather than empirical data. Second, the 30-year observation period may not fully capture the recurrence cycle of megathrust earthquakes, which could span more than a century. Third, this study focused only on temporal probability analysis and did not consider spatial variations in epicenter distribution or depth effects. Despite these limitations, the Poisson model provides a useful and conservative approach for estimating earthquake probabilities in this region, particularly for disaster mitigation planning.

4. CONCLUSION

This study establishes a comprehensive probabilistic seismic hazard profile for the southern offshore East Java region by integrating the Gutenberg–Richter law with a stationary Poisson model, yielding three primary insights. First, the magnitude of completeness was rigorously defined at $M_C = 4.2$ through a corrected Maximum Curvature approach, establishing a robust baseline dataset of 888 mainshock events with a mean magnitude of $\bar{M} = 4.51$. Second, the derived seismic parameters $a = 7.970877$ and $b = 1.195825$ reveal an active, highly productive tectonic environment characterized by a strong predominance of small-to-moderate earthquakes, reflecting continuous stress-release mechanisms within this segment of the Sunda Subduction Zone. Third, long-term forecasting highlights a critical hazard timeline, revealing a striking 92.78% probability of an $M \geq 6.5$ earthquake within the next 50 years, contrasted by a lower but catastrophic 1.06% probability for a multi-century megathrust event $M \geq 8.5$. Beyond the statistical formulations, these findings offer vital practical benchmarks for regional disaster mitigation. The high likelihood of significant seismic activity over the coming decades underscores the necessity of embedding long-term probabilistic hazard estimates directly into local building codes and structural engineering practices. Ultimately, this assessment provides the exact quantitative foundation required by policymakers to enforce strict earthquake-resistant construction standards, optimize coastal tsunami evacuation routes, and strengthen community resilience across the vulnerable coastlines of East Java.

Funding Information
The authors state no funding involved in this research.

Author Contributions Statement
Ajril Abyad Al Haq: Conceptualization, Data curation, Methodology, Formal analysis, Writing – original draft, Visualization, Writing – review & editing.
Eriska Fitri Kurniawati: Supervision, Validation, Writing – review & editing.
All authors discussed the results and contributed to the final manuscript.

Conflict of Interest Statement
The authors state no conflict of interest.

Data Availability
The raw earthquake data are publicly available from the ISC catalog (http://www.isc.ac.uk/iscbulletin/search/catalogue/). The processed data (after declustering and magnitude filtering) supporting the findings of this study are available from the corresponding author upon reasonable request.

REFERENCES

[1] R. Pratama, E. Porcu, and B. Zhou, 'A Markov chain model for earthquake occurrence analysis in Megathrust 4 (M4), Sumatra, Indonesia', *Nat. Hazards*, vol. 121, no. 14, pp. 16779–16797, 2025, doi: https://doi.org/10.1007/s11069-025-07450-6.

[2] W. Wella, R. I. Desanti, and S. Suryasari, 'A Comparative Study of Machine Learning Approaches to Megathrust Earthquake Prediction in Subduction Zones', *J. Appl. Data Sci.*, vol. 6, no. 4, pp. 2421–2435, 2025, doi: https://doi.org/10.47738/jads.v6i4.904.

[3] Y. Asnawi *et al.*, 'Soil classification in a seismically active environment based on join analysis of seismic parameters', *Glob. J. Environ. Sci. Manag.*, vol. 8, no. 3, pp. 297–314, 2022, doi: https://doi.org/10.22034/gjesm.2022.03.01.

[4] A. Arimuko, P.-F. Chen, Y. Serhalawan, and E. Sujarwanto, 'Improved Aftershock of the 2006 Yogyakarta MW 6.4 Earthquake Sequence Using Deep Learning and Its Correlates with Tectonic Setting', *Ann. Geophys.*, vol. 69, p. 9409, 2026.

[5] B. Anggarajati, Y. Yatini, and W. Raharjo, 'Application of K-means clustering and B-value algorithms for analysis of earthquake dangerous zones in Java Island', *Int. J. Adv. Appl. Sci.*, vol. 13, no. 4, pp. 907–915, 2024, doi: http://doi.org/10.11591/ijaas.v13.i4.pp907-915.

[6] F. S. Rahmatullah *et al.*, 'Development of Peak Ground Motion Acceleration Map of Surabaya City based on Probabilistic Seismic Hazard Analysis', in *IOP Conference Series: Earth and Environmental Science*, IOP Publishing, 2025, p. 12032. doi: https://doi.org/10.1088/1755-1315/1458/1/012032.

[7] R. Annisa, M. Jannah, A. H. Saputro, and T. Lestari, 'Enhancing Seismic Data Accuracy: An Advanced Health Diagnosis Method for Seismometers Performance Evaluation', in *Journal of Physics: Conference Series*, IOP Publishing, 2024, p. 12049. doi: https://doi.org/10.1088/1742-6596/2866/1/012049.

[8] M. Wannewitz and M. Garschagen, 'The role of social identities for collective adaptation capacities–general considerations and lessons from Jakarta, Indonesia', *Int. J. Disaster Risk Reduct.*, vol. 100, p. 104194, 2024, doi: https://doi.org/10.1016/j.ijdrr.2023.104194.

[9] P. Zhou and S. Xia, 'Effects of the heterogeneous subducting plate on seismicity: constraints from b-values in the Andaman–Sumatra–Java subduction zone', *Phys. Earth Planet. Inter.*, vol. 304, p. 106499, 2020, doi: https://doi.org/10.1016/j.pepi.2020.106499.

[10] M. D. Petersen *et al.*, 'The 2018 update of the US National Seismic Hazard Model: Overview of model and implications', *Earthq. Spectra*, vol. 36, no. 1, pp. 5–41, 2020, doi: https://doi.org/10.1177/8755293019878199.

[11] M. Fitria and T. Prastowo, 'Seismisitas Jawa Timur Dan Potensi Bahaya Bencana Seismik Terkait', *Inov. Fis. Indones.*, vol. 11, no. 1, pp. 17–27, 2022, doi: https://doi.org/10.26740/ifi.v11n1.p17-27.

[12] M. Afjar and D. A. Maulana, 'Pemodelan Gempa Bumi Di Provinsi Jawa Timur Menggunakan Extreme Value Theory dan Probabilistic Seismic Hazard Analysis', *MATHunesa J. Ilm. Mat.*, vol. 13, no. 3, pp. 261–270, 2025, doi: https://doi.org/10.26740/mathunesa.v13n3.p261-270.

[13] International Seismological Centre, 'International Seismological Centre On-line Bulletin', ISC. Accessed: May 10, 2026. [Online]. Available: https://www.isc.ac.uk/iscbulletin/search/catalogue/

[14] D. Poudyal, N. Nordin, and S. N. A. Roslan, 'Comparative declustering approaches for seismic data: insights from gardner-knopoff, gruenthal, reasenberg, and uhrhammer in the Kathmandu Valley', *Ann. Geophys.*, vol. 68, 2025, doi: https://doi.org/10.4401/ag-9178.

[15] X. Wang, J. Li, A. Feng, and D. Sornette, 'Estimating magnitude completeness in earthquake catalogs: A comparative study of catalog-based methods', *J. Geophys. Res. Solid Earth*, vol. 130, no. 9, p. e2025JB031441, 2025, doi: https://doi.org/10.1029/2025JB031441.

[16] V. A. Pavlenko and A. D. Zavyalov, 'Comparative analysis of the methods for estimating the magnitude of completeness of earthquake catalogs', *Izv. Phys. Solid Earth*, vol. 58, no. 1, pp. 89–105, 2022, doi: https://doi.org/10.1134/S1069351322010062.

[17] J. Woessner and S. Wiemer, 'Assessing the quality of earthquake catalogues: Estimating the magnitude of completeness and its uncertainty', *Bull. Seismol. Soc. Am.*, vol. 95, no. 2, pp. 684–698, 2005, doi: https://doi.org/10.1785/0120040007.

[18] P. Li, C. Chen, Y. Sun, and W. Wang, 'Poisson multi-bernoulli mixture filter for multiple extended object tracking using kolmogorov–smirnov test', *IEEE Sens. J.*, vol. 25, no. 4, pp. 6541–6555, 2025, doi: https://doi.org/10.1109/JSEN.2024.3521436.

[19] K. P. D. Drajati and F. Roshafara, 'Penerapan Proses Poisson Nonhomogen untuk Memprediksi Kejadian Gempa Bumi Jawa Barat', in *Bandung Conference Series: Statistics*, 2025, pp. 713–720. doi: https://doi.org/10.29313/bcss.v5i2.20757.

[20] Y. Yang, N. Dousti Mousavi, Z. Yu, and J. Yang, 'From Poisson observations to fitted negative binomial distribution: Y. Yang et al.', *Stat. Pap.*, vol. 67, no. 3, p. 62, 2026, doi: https://doi.org/10.1007/s00362-026-01842-x.

[21] K. Aki, 'Maximum likelihood estimate of b in the formula log N= a− bM and its confidence limits', *Bull. Earthq. Res. Inst. Univ. Tokyo*, vol. 43, pp. 237–239, 1965.

[22] A. M. Lombardi, 'A statistical framework for detection of b-value anomalies in Italy', *Geophys. J. Int.*, vol. 237, no. 2, pp. 729–740, 2024, doi: https://doi.org/10.1093/gji/ggae068.

[23] B. Gutenberg and C. F. Richter, 'Frequency of earthquakes in California', 1944.

[24] P. Adetokunbo *et al.*, 'Geostatistical Analysis for Magnitude Scale Conversion and Gutenberg-Richter Parameter Estimation: Insights from Regional Seismicity of

Nubian-Eurasian Plate Boundary Region', *J. Geosci. Environ. Prot.*, vol. 13, no. 7, pp. 230–248, 2025, doi: https://doi.org/10.4236/gep.2025.137014.

[25] C. A. Cornell, 'Engineering seismic risk analysis', *Bull. Seismol. Soc. Am.*, vol. 58, no. 5, pp. 1583–1606, 1968.

[26] E. H. Field, K. R. Milner, and K. A. Porter, 'Risk implications of Poisson assumptions and declustering inferred from a fully time-dependent earthquake forecast', *Earthq. Spectra*, vol. 41, no. 3, pp. 1977–1997, 2025, doi: https://doi.org/10.1177/87552930251340677.